Title	Efficient dehalogenation of polyhalomethanes and production of strong acids in aqueous environments: Water-catalyzed O-H-insertion and HI-elimination reactions of isodiiodomethane (CH 2I-I) with water
Author(s)	Kwok, WM; Zhao, C; Guan, X; Li, YL; Du, Y; Lee Phillips, D
Citation	Journal Of Chemical Physics, 2004, v. 120 n. 19, p. 9017-9032
Issued Date	2004
URL	http://hdl.handle.net/10722/42362
Rights	Creative Commons: Attribution 3.0 Hong Kong License

Efficient dehalogenation of polyhalomethanes and production of strong acids in aqueous environments: Water-catalyzed O–H-insertion and HI-elimination reactions of isodiiodomethane (CH_2I–I) with water

Wai Ming Kwok, Cunyuan Zhao,[a] Xiangguo Guan, Yun-Liang Li, Yong Du, and David Lee Phillips[b]
Department of Chemistry, University of Hong Kong, Pokfulam Road, Hong Kong, China

(Received 10 September 2003; accepted 19 February 2004)

A combined experimental and theoretical study of the ultraviolet photolysis of CH_2I_2 in water is reported. Ultraviolet photolysis of low concentrations of CH_2I_2 in water was experimentally observed to lead to almost complete conversion into $CH_2(OH)_2$ and 2HI products. Picosecond time-resolved resonance Raman spectroscopy experiments in mixed water/acetonitrile solvents (25%–75% water) showed that appreciable amounts of isodiiodomethane (CH_2I–I) were formed within several picoseconds and the decay of the CH_2I–I species became substantially shorter with increasing water concentration, suggesting that CH_2I–I may be reacting with water. *Ab initio* calculations demonstrate the CH_2I–I species is able to react readily with water via a water-catalyzed O–H-insertion and HI-elimination reaction followed by its $CH_2I(OH)$ product undergoing a further water-catalyzed HI-elimination reaction to make a $H_2C{=}O$ product. These HI-elimination reactions produce the two HI leaving groups observed experimentally and the $H_2C{=}O$ product further reacts with water to produce the other final $CH_2(OH)_2$ product observed in the photochemistry experiments. These results suggest that CH_2I–I is the species that reacts with water to produce the $CH_2(OH)_2$ and 2HI products seen in the photochemistry experiments. The present study demonstrates that ultraviolet photolysis of CH_2I_2 at low concentration leads to efficient dehalogenation and release of multiple strong acid (HI) leaving groups. Some possible ramifications for the decomposition of polyhalomethanes and halomethanols in aqueous environments as well as the photochemistry of polyhalomethanes in the natural environment are briefly discussed. © *2004 American Institute of Physics.* [DOI: 10.1063/1.1701699]

I. INTRODUCTION

The photochemistry and chemistry of polyhalomethanes have been of interest in atmospheric chemistry, environmental chemistry, synthetic chemistry, and chemical reaction dynamics. Polyhalomethanes such as CH_2I_2, CH_2BrI, $CHBr_3$, CCl_4, $CFCl_3$, and others have been observed in the atmosphere and are thought to be important sources of reactive halogens in the atmosphere.[1–8] The photochemistry of CH_2I_2 and CH_2BrI was recently linked to the formation of IO produced during localized ozone-depletion events in the marine boundary layer of the troposphere.[7,8] Both gas-phase and condensed-phase photochemistry and chemistry are recognized to be important for properly describing reaction processes in the atmosphere.[9–21] There has recently been much interest in reactions associated with the activation of halogens in aqueous sea-salt particles.[10–21] Polyhalomethanes like CH_2I_2 have also been used as reagents for cyclopropanation of olefins and diiodomethylation of carbonyl compounds.[22–41] Examples include cyclopropanation of olefins by ultraviolet photolysis of CH_2I_2 in the presence of the olefins[23,32,33,35] or via Simmons–Smith-type reagents.[22,28–30,41] Polyhalomethane molecules are also attractive to study fundamental photodissociation processes in chemical reaction dynamics.[42–69]

Gas-phase ultraviolet photolysis of polyhalomethanes generally leads to one direct carbon–halogen bond cleavage.[42–58] Time-of-flight photofragment spectroscopy results indicate that the polyatomic photofragment typically receives a large amount of excitation of its internal degrees of freedom (vibration and rotation).[44,47–51] Gas- and solution-phase resonance Raman experiments for several polyhalomethanes showed that photodissociation typically had a noticeable multidimensional character and Franck–Condon region dynamics qualitatively consistent with a semirigid radical description of the dissociation process.[59–69]

Ultraviolet excitation of polyhalomethanes in condensed phases leads to photoproducts with characteristic transient absorption bands in the ultraviolet and visible regions which were assigned to a number of different species.[70–82] Femtosecond transient absorption measurements showed that these photoproducts are mainly formed by geminate recombination of the photofragments within the solvent cage.[77–82] Maier and co-workers first assigned the isodiiodomethane (CH_2I–I) photoproduct as the one responsible for these intense transient absorption spectra based on IR vibrational frequencies observed in low-temperature matrices and a comparison to *ab initio* frequencies.[73,74] Tarnovsky *et al.*[79]

[a]Permanent address: Department of Chemistry, Northwest Normal University, Lanzhou 730070, China.
[b]Author to whom correspondence should be addressed.

observed similar transient absorption spectra in room-temperature solutions and assigned these bands to be due to the CH_2I–I photoproduct. This was subsequently confirmed by time-resolved resonance Raman (TR^3) experiments.[85,88] A number of isopolyhalomethane photoproducts have been observed after ultraviolet excitation of polyhalomethanes in condensed-phase environments.[73,74,77–92]

We explored the chemical reactivity of isopolyhalomethanes towards olefins theoretically and experimentally.[87,89,93–98] Density functional theory (DFT) calculations revealed that the CH_2I–I species can readily react with ethylene to produce a cyclopropane product and I_2 leaving group with a barrier of only 2.9 kcal/mol, but the CH_2I radical and CH_2I^+ cations have much more difficult pathways to make cyclopropanated products.[93,94] TR^3 experiments showed that CH_2I–I reacts with cyclohexene on the 5–10-ns time scale to make an I_2 leaving group that immediately complexes with the solvent to make an I_2:cyclohexene complex[95] under conditions similar to those that observed significant formation of the cyclopropanated product of cyclohexene (norcarane) after ultraviolet photolysis of CH_2I_2.[23] These experimental and theoretical results indicated that CH_2I–I is the carbenoid species mostly responsible for the cyclopropanation of olefins when the ultraviolet photolysis of CH_2I_2 method is used and a reaction mechanism was proposed.[93–95] Other isopolyhalomethanes were found to also behave as carbenoids with varying reactivity to olefins.[87,89,94,97] The chemical reactivity of CH_2I–I was observed to be similar to that of singlet methylene towards C═C bonds in producing cyclopropanated products with high stereospecificity and little C–H-insertion products.[93,99,100] Carbenes and carbenoids may also react with O–H bonds in water and alcohols.[101–110] Examples include the O–H-insertion reactions of singlet methylene[101–104,106–108] and dichlorocarbene ($:CCl_2$) [109,110] with water to produce CH_3OH and $CHCl_2OH$ products. Picosecond TR^3 experiments[111] have recently observed the formation and decay of CH_2I–I in largely aqueous solvents, and the shorter lifetimes observed for increasing concentration of O–H bonds suggested that CH_2I–I reacts with O–H bonds in alcohols and/or water. This led us to begin to explore the chemical reactivity of isopolyhalomethanes towards water.[112] Preliminary MP2 calculations indicated that CH_2I–I could react with one water molecule to produce O–H-insertion products and an HI leaving group.[112] The O–H-insertion reactions of CH_2I–I with water were found to be catalyzed by a second water molecule[112] in a manner similar to that previously found for the reaction of dichlorocarbene with two water molecules.[109,110] These results suggested that isopolyhalomethanes may undergo O–H-insertion reactions with water and release a strong acid leaving group.

In this paper, we report a more comprehensive combined experimental and theoretical study of the ultraviolet photolysis of CH_2I_2 in water and reactions of isodiiodomethane (CH_2I–I) with water. Ultraviolet photolysis of CH_2I_2 with low concentrations in water was found to produce almost complete conversion into $CH_2(OH)_2$ and 2HI products. Picosecond time-resolved resonance Raman (ps-TR^3) spectroscopy experiments in mixed water/acetonitrile solvents (25%–75% water) observed that isodiiodomethane (CH_2I–I) was formed within several picoseconds. The decay of the CH_2I–I species became significantly faster with increasing water concentration and could be indicative of CH_2I–I reacting with water. *Ab initio* calculations showed that CH_2I–I reacts easily with water via a water-catalyzed O–H-insertion and HI-elimination reaction followed by the $CH_2I(OH)$ product undergoing a further water-catalyzed HI-elimination reaction to make an H_2C═O product that reacts with water to produce the final products experimentally observed. These indicate that CH_2I–I is the species that reacts with water to produce the $CH_2(OH)_2$ and 2HI products observed experimentally. We briefly discuss some implications for the photochemistry of polyhalomethanes in aqueous environments.

II. EXPERIMENTAL AND COMPUTATIONAL DETAILS

A. Photochemistry experiments

Sample solutions were prepared using commercially available CH_2I_2 (99%), $^{13}CH_2I_2$, formaldehyde in water (reagent grade), D_2O 99.9% D, and de-ionized water. Samples of about 1×10^{-4} Mol CH_2I_2 in water were housed in a 10-cm-path-length glass holder with quartz windows. The sample solution was excited by an about 3-mJ 266-nm unfocused laser beam from the fourth harmonic of a Nd:YAG laser in the laser photolysis experiments. The sample was excited by a Hg lamp placed about 5 cm from the quartz window of the sample holder with a 280-nm-long pass filter inserted between the Hg lamp and the quartz window to prevent excitation by high-energy photons in the lamp photolysis experiments. The absorption spectra for the photolyzed samples were obtained using a 1-cm UV grade cell and a Perkin Elmer Lambda 19 UV/VIS spectrometer. The *p*H of the photolyzed samples was monitored using an THERMO Orion 420A *p*H meter equipped with a 8102BN combination *p*H electrode that was calibrated with 7.00-*p*H and 4.01-*p*H buffer solutions. Both ^{13}C and ^{1}H NMR spectra were obtained using a Bruker Advance 400 DPX spectrometer and $\phi=5$ mm sample tubes at room temperature. The $^{13}CH_2I_2$ concentration was $\sim$1.2 mM in D_2O and the chemical shifts were referenced to the TMS signal (set as 0 ppm). IR spectra were acquired using a Bio-rad FTS 165 spectrometer using $\sim$20-μm sample thickness and CaF_2 windows for the sample holder. Spectra were obtained for the sample in H_2O solvent, the H_2O solvent, and a base-line background. The H_2O solvent spectrum and the base-line background spectrum were subtracted from the sample in H_2O spectrum in order to find the resulting sample spectrum.

B. Picosecond time-resolved resonance Raman (ps-TR^3) spectroscopy experiments

A femtosecond mode-locked Ti:sapphire laser (Spectra-Physics, Tsunami) pumped by the second harmonic of a Nd:YVO4 laser (Spectra-Physics, Millennia V) was used as the seed laser for an amplified laser system composed of a picosecond regenerative amplifier (Spectra-Physics, Spitfire) pumped by the second harmonic of a Nd:YLF laser (Spectra-Physics, Evolution X). The output from the regenerative am

plifier system (800 nm, 1 ps, 1 kHz) was frequency doubled and tripled by KDP crystals to make the probe (400 nm) and pump (267 nm) laser beams. The time zero delays between the pump and probe laser beams were obtained by employing fluorescence depletion of trans-stilbene. The optical delay between the pump and probe beams was varied to a position where the depletion of the stilbene fluorescence was halfway to the maximum fluorescence depletion by the probe laser. The time zero measured between the pump and probe beams had an estimated accuracy of ± 0.5 ps and a typical cross correlation of about 1.5 ps [full width at half maximum (FWHM)]. In order to use the laser beams more effectively and noting that the rotational reorientation dynamics are much faster than the dynamics examined in this investigation, parallel polarization of the pump and probe laser beams was used in the ps-TR^3 experiments rather than the magic angle polarization. The pump and probe beams were lightly focused onto a thin-film stream ($\sim$500 μm thick) of the sample solution. Typical pulse energies and spot sizes at the sample were 15 μJ and 250 μm for the pump beam and 8 μJ and 150 μm for the probe beam. An ellipsoidal mirror with $f/1.4$ and a backscattering geometry was used to acquire the Raman scattered light from the sample and image the light through the entrance slit of a 0.5-m spectrograph. A 1200-groove/mm-ruled grating blazed at 250 nm in the spectrograph dispersed the Raman light onto a liquid-nitrogen-cooled charge-coupled-device (CCD) detector.

Each spectrum presented here was found from subtraction of a scaled probe-before-pump and scaled net solvent measurements from a pump–probe spectrum so as to subtract out the CH_2I_2 ground-state Raman bands and residual solvent Raman bands, respectively. The known Raman shifts of the solvent Raman bands were used to calibrate the spectra with an estimated uncertainty of ± 5 cm^{-1} in absolute frequency. Commercially available 99% CH_2I_2 and spectroscopic grade acetonitrile solvent were used as is to produce half-liter volume CH_2I_2 (7×10^{-3} mol dm^{-3}) samples prepared in water/acetonitrile mixed solvents (25%, 50%, and 75% water). During the experimental segments, the samples exhibited $<$3% degradation as found from the UV absorption spectra acquired before and after the TR^3 measurement.

C. *Ab initio* calculations

The MP2 method was employed to examine the CH_2I–I+$n H_2O$ (where $n=0,1,2,3$) and $CH_2I(OH)+nH_2O$ (where $n=0,1,2,3,4$) reactions. Both the geometry optimization and frequency calculations (analytically) were done with the 6-31G* basis set for all C, H, and O atoms and the 6-311G** basis set for iodide atoms. The frequency calculations for the reaction system of CH_2I–I+$3H_2O$ were performed numerically due to limited computer resources. All calculations made use of the GAUSSIAN 98 program suite.[113] IRC calculations were done to confirm the transition states connected the appropriate reactants and products.[114] The Cartesian coordinates, total energies, and vibrational zero-point energies for the calculated structures are provided in the supporting information (see Ref. 115).

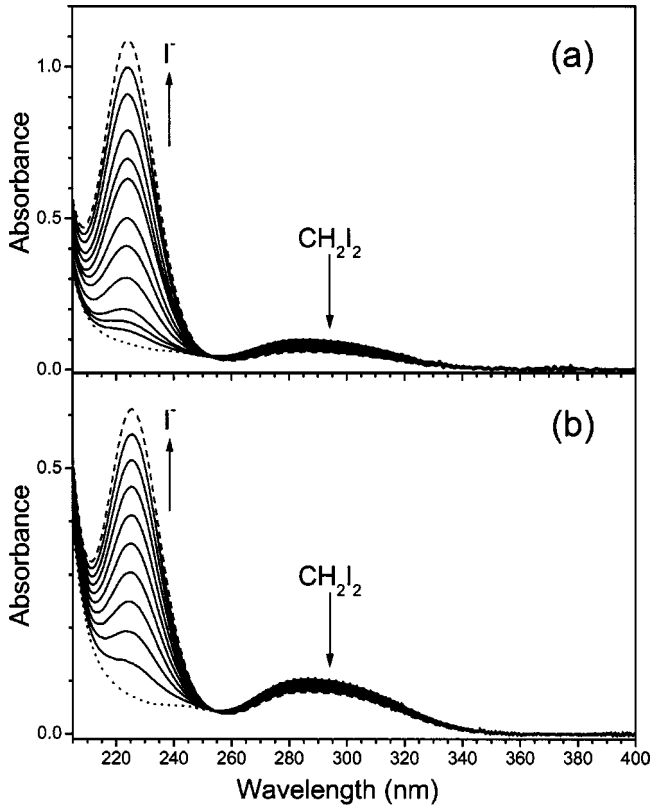

FIG. 1. Absorption spectra acquired after varying times of photolysis of 1.0×10^{-4} mol CH_2I_2 in water using either 266-nm light obtained from a nanosecond Nd:YAG laser (a) or wavelengths $>$280 nm obtained from a low-pressure Hg lamp (b). The parent CH_2I_2 absorption bands in the 280–320-nm region decrease in intensity as a new absorption band due to I^- appears at about 220 nm with a clear isobestic point at 253 nm. The I^- absorption band is essentially identical to that found for KI salt dissolved in water (not shown).

III. RESULTS AND DISCUSSION

A. CH_2I_2 ultraviolet photolysis in water and product analysis

Figure 1 displays ultraviolet and visible spectra obtained following varying times for 266-nm laser photolysis (a) and Hg lamp excitation with wavelengths $>$280 nm (b) of 1×10^{-4} mol CH_2I_2 in water solution. Inspection of Fig. 1 shows that the absorption bands due to CH_2I_2 in the 280–300-nm region decrease in intensity while those due to the I^- ion in the 220-nm region increase in intensity as the time for photolysis increases. There is a clear isobestic point at about 253 nm, and this indicates the I^- is directly produced from the CH_2I_2 parent molecule. We measured the molar absorption extinction coefficients for CH_2I_2 and I^- in water and found them to be $\varepsilon_{288\,nm}=1129$ cm^{-1} mol^{-1} and $\varepsilon_{226\,nm}=13\,240$ cm^{-1} mol^{-1}, respectively. The pH of the sample solution was measured for each of the UV–VIS spectra acquired during the photochemistry experiments shown in Fig. 1 in order to check for any correlation of the pH changes with photolysis of CH_2I_2. The measured molar absorption extinction coefficients for CH_2I_2 and I^- were used to find the concentrations of these species for each of the photolysis times from the UV–VIS spectra shown in Fig. 1. Plots of $\Delta[I^-]$ versus $-\Delta[CH_2I_2]$ were produced and are shown in

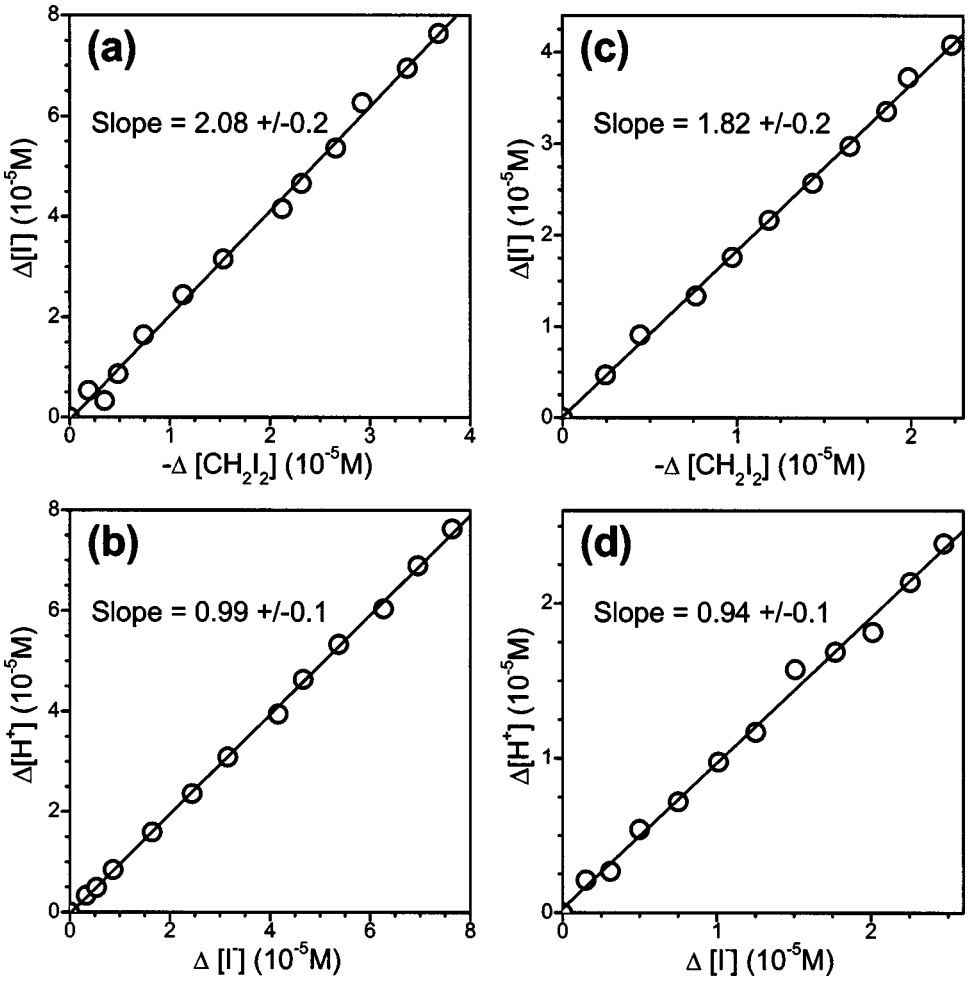

FIG. 2. (a) and (c) Plots of $\Delta[I^-]$ vs $-\Delta[CH_2I_2]$ derived from the spectra of Fig. 1 are shown. The increase in $[I^-]$ versus the decrease in $[CH_2I_2]$ during the photochemistry experiments exhibits a linear relationship with a slope of about 2 and indicates a release of two I^- products. (b) and (d) Plots of $\Delta[H^+]$ derived from the *p*H measurements versus the changes in the $[I^-]$ concentrations. These plots of $\Delta[H^+]$ vs $\Delta[I^-]$ display an excellent linear correlation with a slope of about 1. The data for (a) and (b) are associated with the spectra of Fig. 1(a) obtained using 266-nm light from a nanosecond Nd:YAG laser. The data of (c) and (d) are associated with the spectra of Fig. 1(b) obtained using cw excitation from a low-pressure Hg lamp.

(a) and (c) of Fig. 2. The increase in $[I^-]$ versus the decrease in $[CH_2I_2]$ during the photochemistry experiments shown in Fig. 2 reveals a linear relationship with a slope of about 2 for both types of photochemistry experiments. This indicates that ultraviolet photolysis of CH_2I_2 in water at low concentration releases two I^- products. Plots of the changes in the $[H^+]$ concentrations derived from the *p*H measurements were plotted versus the changes in the $[I^-]$ concentrations and these are shown in (b) and (d) of Fig. 2. The plots of $\Delta[H^+]$ vs $\Delta[I^-]$ show an excellent linear correlation and a slope of about 1 in both cases. These results for the UV–VIS and *p*H photochemistry experiments shown in Figs. 1 and 2 indicate that ultraviolet photolysis of CH_2I_2 in water at low concentration releases two H^+ and two I^- products (e.g., two HI products that immediately dissociate to two H^+ and two I^- in water solvent).

In order to learn more about the fate of the carbon atom from the CH_2I_2 parent molecule following 266-nm photolysis, we next used a carbon-13-labeled sample of CH_2I_2. We then repeated the 266-nm photolysis experiments and obtained ^{13}C-NMR spectra before, during, and after complete photolysis of $^{13}CH_2I_2$ in D_2O solvent as shown in Figs. 3(a)–3(c). Inspection of Fig. 3 shows that before photolysis there is only the parent $^{13}CH_2I_2$ band at about -63.9 ppm relative to the TMS reference band ~ 0 ppm [Fig. 3(a)]. During photolysis, this parent $^{13}CH_2I_2$ band decreases in intensity and a new photoproduct band [see Fig. 3(b)] appears at about 82.5 ppm. After complete photolysis (e.g., the UV–VIS spectrum shows that the CH_2I_2 parent absorption bands have been converted into the I^- absorption band), the parent $^{13}CH_2I_2$ band has disappeared and only the photoproduct band at about 82.5 ppm is left. The characteristic 82.5-ppm ^{13}C-NMR band associated with the photoproduct produced after $^{13}CH_2I_2$ photolysis in D_2O is in agreement with that reported in the literature for $CH_2(OH)_2$ in aqueous solution taking into account the different reference molecules used in the ^{13}C-NMR experiments.[116] We tentatively assign the 82.5-ppm ^{13}C-NMR band to a $^{13}CH_2(OD)_2$ photoproduct. ^{1}H-NMR spectra were also obtained under similar conditions as the ^{13}C-NMR experiments (see Fig. S1 in Ref. 115) and provide further evidence for the $^{13}CH_2(OD)_2$ photoproduct being produced after ultraviolet photolysis of $^{13}CH_2I_2$ in D_2O solvent.[116] Similar results were found using excitation by the Hg lamp with wavelengths >280 nm. Authentic samples of $CH_2(OH)_2$ can be easily made by dissolving a small amount of formaldehyde in water.[116–119] We obtained IR spectra of a small amount of formaldehyde in water and this is shown in Fig. 3(d). We then obtained IR spectra before and after 266-nm photolysis of CH_2I_2 in water and obtained a difference spectrum of the photoproduct produced and this is shown in Fig. 3(e). This spectrum is essentially identical to that found for $CH_2(OH)_2$ produced by dissolving formalde-

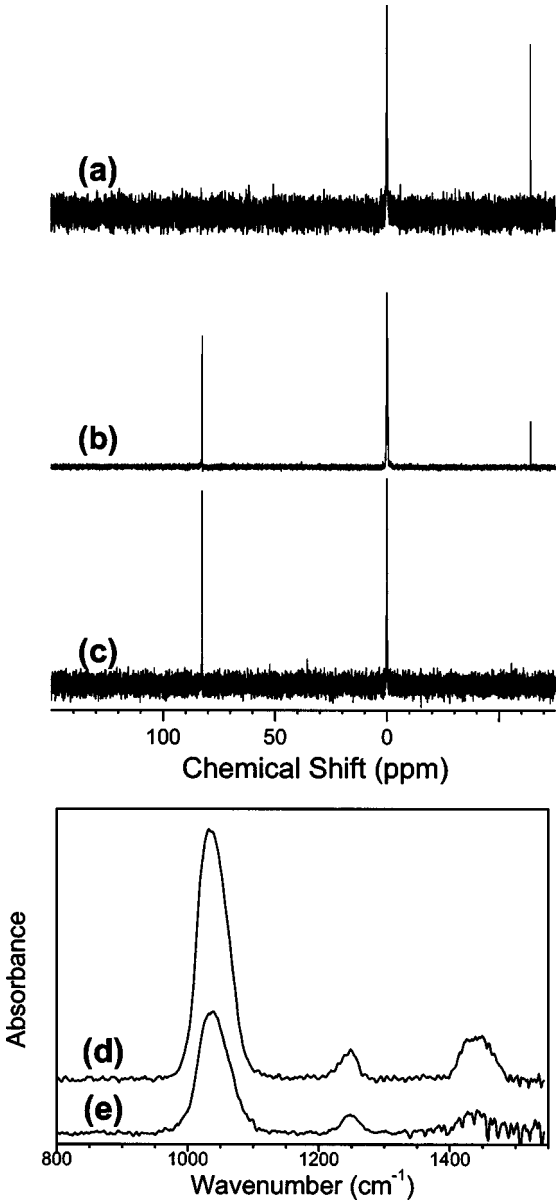

FIG. 3. (Top) ^{13}C-NMR spectra obtained before (a), during (b), and after (c) complete photolysis of $^{13}CH_2I_2$ in D_2O solvent. The parent $^{13}CH_2I_2$ band appears at -63.9 ppm and the ^{13}C-labeled TMS reference band is at 0 ppm. Photolysis converts the parent $^{13}CH_2I_2$ band into a new photoproduct band at 82.5 ppm that is assigned to $^{13}CH_2(OD)_2$ (see text for more details). (Bottom) IR spectrum obtained for a small amount of formaldehyde in water (d). IR difference spectrum of the photoproduct produced from 266-nm photolysis of CH_2I_2 in water (e). This was found by taking IR spectra before and after 266-nm photolysis of CH_2I_2 in water and then obtaining a difference spectrum. This spectrum is essentially identical to that found for $CH_2(OH)_2$ produced by dissolving formaldehyde in water and confirms that a $CH_2(OH)_2$ product is produced following ultraviolet photolysis of CH_2I_2 in water. This is consistent with the photochemistry NMR results.

hyde in water. The results of Figs. 3(d) and 3(e) confirm that a $CH_2(OH)_2$ product is produced following ultraviolet photolysis of CH_2I_2 in water and this is consistent with the NMR photochemistry experiments shown in Fig. 3 and S1 that also observed the ^{13}C-NMR and ^{1}H-NMR spectra of a $^{13}CH_2(OD)_2$ photoproduct.

Combining the preceding experimental photochemistry results indicates that ultraviolet photolysis of CH_2I_2 at low concentration in water leads to the following overall reaction:

$$CH_2I_2 + h\nu + nH_2O \rightarrow CH_2(OH)_2 + 2HI + (n-2)H_2O. \quad (1)$$

The experimental results shown in Figs. 1–3 also indicate that this reaction can convert almost all of the parent CH_2I_2 compound under low-concentration conditions into $CH_2(OH)_2$ and 2HI products with no other discernible reaction products. We made measurements to estimate the photoquantum yield for reaction (1) and found a value of about 0.35 ± 0.1 (see supporting information for a description of the photoquantum yield measurement).[115]

It is important to note that the photochemistry experiments done with an unfocused nanosecond laser beam and a Hg lamp source of light gave essentially the same results for the production of the photoproducts for low concentrations of CH_2I_2 in water. This indicates that the photoproducts observed are due to a single-photon process. We also note that essentially the same results were obtained when the concentrations were varied from 0.5×10^{-4} to 2×10^{-4} mol (see Fig. S2 in the supporting information).[115] Although the concentration could not be varied much due to a combination of the low solubility of CH_2I_2 in water and the ability to obtain clear absorption spectra, there does not appear to be any concentration effects on the photochemistry at low concentrations $<2\times10^{-4}$ mol. We note that previous photochemistry experiments on other polyhalomethanes like $CHCl_2Br$, $CHBr_2Cl$, and $CHBr_3$ also found that Hg lamp excitation (mainly 253.7 nm in these experiments) at low concentrations ($<10^{-6}$ mol) in water led to complete conversion of the organic halogen present in the polyhalomethanes into their halide ions (Cl^- and/or Br^-) with a photoquantum yield of about 0.43.[120] Our present results for CH_2I_2 at relatively low concentrations are consistent with these previous results for both the conversion of the organic halogens into their halide ions with an appreciable quantum yield via a one-photon process. These results for CH_2I_2, $CHCl_2Br$, $CHBr_2Cl$, and $CHBr_3$ suggest that it may be common for ultraviolet excitation of many polyhalomethanes at low concentrations in water to be converted quantitatively into halide ions.

We do note that at higher concentrations of CH_2I_2 in water/acetonitrile or acetonitrile solutions one easily observes absorption bands due to I_2^- and I_3^- secondary products formed from I^- and I products produced from different molecules in the solution (presumably via diffusion controlled reactions). For example, 266-nm photolysis of about 10^{-2} mol CH_2I_2 in acetonitrile was found to produce absorption bands due to I^-, I_2^-, and I_3^- on the microsecond time scale (see Fig. 4 of Ref. 121).[121] At low concentrations the initially formed CH_2I and I radical fragments appear to be mainly scavenged by the radical from the same parent molecule and there is little scavenging by radicals from other parent molecules because the parent molecules are very far apart from one another. This would lead mostly to formation of either the very reactive isomer species that undergoes reaction with water to produce the halide ions or the parent molecule. This is consistent with the nearly quantitative con-

version of organic halogens in CH_2I_2, $CHCl_2Br$, $CHBr_2Cl$, and $CHBr_3$ observed here and in Ref. 120 following ultraviolet excitation of low concentrations of polyhalomethanes in water. However, at high concentrations there is appreciable scavenging by either the initial photofragments or reaction products derived from other parent molecules since the parent molecules are much closer to one another. Thus the initial fragments and/or reaction products are more likely to be scavenged by partners originally from other parent molecules at high concentrations and form products like I_2, CH_2ICH_2I, I_2^- I_3^- that are not formed in appreciable amounts at low concentrations of parent molecules.

What species produced by the ultraviolet photolysis of CH_2I_2 in aqueous solutions can lead to efficient reaction(s) to produce $CH_2(OH)_2$ and 2HI products? We recently observed that photolysis of CH_2I_2 in largely aqueous solutions leads to appreciable formation of CH_2I–I photoproduct with the lifetime of CH_2I–I becoming substantially shorter in mixed aqueous solvents as the amount of O–H bonds present in the solvent system increases.[111] This suggests that the CH_2I–I photoproduct could be reacting with the O–H bonds of the solvent molecules. We have continued to investigate the chemical reactivity of CH_2I–I towards water as detailed in the next two sections.

B. Picosecond time-resolved resonance Raman experiments

Since our previous ps-TR^3 studies of CH_2I_2 in largely aqueous solvents[111] did not explicitly vary the concentration of water to determine its effect on the lifetime of the isodiiodomethane (CH_2I–I) species, we have done this in our present study. Figure 4 presents ps-TR^3 spectra obtained for the photoproducts produced after 267-nm photolysis of CH_2I_2 in water/acetonitrile mixed solvents with water concentrations of 25%, 50%, and 75% using a 400-nm probe wavelength. The spectra obtained in the 50% water/50% acetonitrile solvent system is in excellent agreement with the ones previously found in Ref. 111. The Raman bands observed in Fig. 4 are readily assigned to the CH_2I–I species as discussed previously in Refs. 85, 88, and 111. Examination of Fig. 4 reveals that the CH_2I–I photoproduct Raman bands appear within several picoseconds and then decay on the hundreds of picosecond to ns time scale. The Raman band near 715 cm^{-1} assigned to the fundamental nominal C–I stretch mode (ν_3) was integrated at different time delays so as to inspect the kinetics of the growth and decay of the CH_2I–I species. Figure 5 show plots of the relative integrated area of the ν_3 Raman band from 0 to 6000 ps in the water/acetonitrile-mixed solvents. The relative integrated areas of the ν_3 Raman bands were fit to a simple function (the solid, dashed, and dotted lines in Fig. 6 represent these fits):

$$I(t)=Ae^{-t/t_1}-Be^{-t/t_2}, \tag{2}$$

where $I(t)$ is the relative integrated area of the ν_3 Raman band, t is the time, t_1 is the decay time constant of the ν_3 Raman band, t_2 is the growth time constant of the ν_3 Raman band, and A and B are constants. The fits to the data in Fig. 5 found that the CH_2I–I photoproduct had time constants

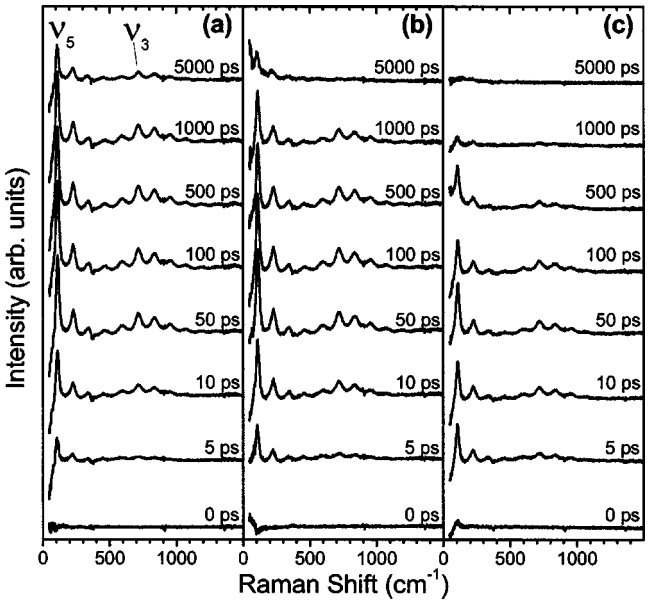

FIG. 4. Stokes ps-TR^3 spectra obtained following 267-nm photolysis of CH_2I_2 in acetonitrile/water mixed solvents using a 400-nm probe excitation wavelength. Spectra in (a), (b), and (c) were obtained in 25%, 50%, and 75% water, respectively. Spectra were acquired at varying pump and probe time delays as indicated to the right of each spectrum. Assignments are indicated for some of the larger isodiiodomethane (CH_2I–I) Raman bands. See Refs. 85, 88, and 111 for details of the Raman band assignments to isodiiodomethane (CH_2I–I).

(t_2) of 8, 6, and 4 ps for its growth and (t_1) of 4640, 1860, and 680 ps for its decay in the mixed solvents with water concentrations of 25%, 50%, and 75%, respectively. The CH_2I–I Raman bands decay with the lifetime decreasing significantly as the water concentration increases, suggesting CH_2I–I may be reacting with the water molecules.

A recently reported study found the CH_2I–I species decays with a rate constant of 4.3×10^6 s^{-1} in pure acetonitrile solvent.[121] This decay was attributed to CH_2I–I decomposing into a CH_2I radical and I atom accompanied by some

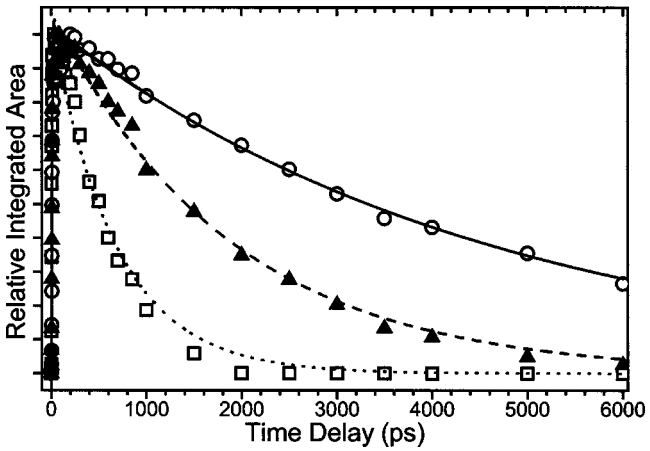

FIG. 5. Plots of the relative integrated area of the ν_3 Raman band of CH_2I–I at different delay times (from 0 ps to 6000 ps) obtained in 25% water/75% acetonitrile (open circles), 50% water/50% acetonitrile (solid triangles), and 75% water/25% acetonitrile (open squares) solvents, respectively. The solid line (25% water/75% acetonitrile), dashed line (50% water/50% acetonitrile), and dotted line (75% water/25% acetonitrile) represents least-squares fits to the data (see text for more details).

decay into I^- product.[121] The rate of decay of CH_2I–I in the presence of water (25%–75% in the spectra shown in Fig. 4) is almost two to three orders of magnitude faster than in pure acetonitrile solvent and appears more consistent with a reaction with water molecules than a change in solvent properties like the dielectric constant.[121] Some indirect support for this comes from the fact that the decay of CH_2I–I in pure methanol $k=(1.3\times10^8\ s^{-1})$ was found to be more than two orders of magnitude faster[121] than in pure acetonitrile ($k=4.3\times10^6\ s^{-1}$) even though the dielectric constants of these solvents are similar (33.1 for methanol and 38.8 for acetonitrile at 20 °C). It is interesting that the decay of CH_2I–I in methanol ($k=1.3\times10^8\ s^{-1}$) is similar to that for 25%–50% water in acetonitrile solvent that had measured time constant of 4640–1860 ps and corresponding rate constants of $k=2.2\times10^8$ and $5.4\times10^8\ s^{-1}$, respectively. This similarity would be consistent with the CH_2I–I species undergoing O–H-insertion reactions with the O–H bond of methanol and the O–H bonds of water, while there is no possible O–H-insertion reaction for the acetonitrile solvent. This would help explain why the decomposition of CH_2I–I is much slower in acetonitrile solvent than in pure methanol or mixed water/acetonitrile solvents.

The hypothesis that CH_2I–I reacts with the O–H bonds of water and alcohols is consistent with the carbenoid behavior of isodiiodomethane (CH_2I–I) and other isopolyhalomethanes as shown towards carbon double bonds to make cyclopropanated products.[87,89,93–95,97] The chemical reactivity of CH_2I–I is similar to that of singlet methylene towards C═C bonds in making cyclopropanated products with high stereospecificity and little C–H-insertion products.[93,99,100] Carbenes and carbenoids like singlet methylene[101–104,106–108] and dichlorocarbene ($:CCl_2$)[109,110] can react with O–H bonds of water to produce CH_3OH and $CHCl_2OH$ products and can also react with O–H bonds in alcohols.[101–110] This and the recent direct observation of the isobromoform O–H-insertion reaction with water to produce a $CHBr_2OH$ reaction product[122] indicates that CH_2I–I would likely also undergo a similar O–H-insertion reaction with water and methanol in so far as CH_2I–I has a chemical reactivity similar to isobromoform and other carbeoid species. We have done further work on the O–H-insertion reaction of CH_2I–I with water and the fate of its reaction product CH_2IOH by examining their reactions as a function of water molecules explicitly included in the reaction system and these results are presented in the next section.

C. *Ab initio* calculations for the reactions of CH_2I–I $+nH_2O$ (where $n=1,2,3$) and $CH_2I(OH)+nH_2O$ (where $n=0,1,2,3,4$): Building water-catalyzed reactions one molecule at a time

Figures 6 and 7 present the optimized geometry with selected bond length and bond angle parameters and Fig. 8 presents schematic diagrams of the relative energy profiles (in kcal/mol) obtained from MP2 calculations (using the 6-31G* basis set for all C, H, and O atoms and the 6-311G** basis set for iodide atoms) for the reactants, reactant complexes, transition states, product complexes, and products for the reactions of CH_2I–I$+nH_2O$ (where $n=1,2,3$) and $CH_2I(OH)+nH_2O$ (where $n=0,1,2,3,4$).

1. Reactions of CH_2I–I$+nH_2O$ (where $n=0,1,2,3$)

Figure 6 shows that there are some systematic trends in the structures of the reactant complexes (RCs) and transition states (TSs) as the number of H_2O molecules involved in the CH_2I–I$+nH_2O$ (where $n=0,1,2,3$) reaction increases. The C–I bond length decreases (from 1.979 Å in RC1 to 1.973 in RC3), the I–I bond length increases (from 3.058 Å in RC1 to 3.088 Å in RC3), and the O···H–C distance decreases (from 2.441 Å in RC1 to 2.070 Å in RC3) in the RCs as the number of H_2O molecules increases. Similarly, the C–I bond length decreases from 1.968 Å in TS1 to 1.954 Å in TS3, the I–I bond length decreases from 3.368 Å in TS1 to 3.234 Å in TS3 and the O···H–C distance increases from 2.321 (2.386) Å in TS1 to 2.432 Å in TS3. The I–I–C angle increases from 95.5° in TS1 to 117.1° in TS3 and the C–O bond length increases from 2.111 Å in TS1 to 2.386 Å in TS3. These changes in the RC and TS structures as the number of H_2O molecules increases can be largely attributed to solvation of the terminal I atom with more hydrogen-bonding-like interactions while also interacting with the CH_2 group of the CH_2I–I species via the O···H–C interaction.

The changes in structure in Fig. 6 occurring as the RCs proceed to the TSs indicate that the C–I bond becomes modestly stronger, the I–I bond noticeably weakens, and the C–O bond becomes partially formed. These changes are accompanied by the $I^2\cdots H$ interactions becoming somewhat stronger, which is consistent with some H–I bond formation. The changes observed as the RCs go to the TSs are consistent with an O–H-insertion and HI-elimination reaction taking place to form the $CH_2I(OH)$ product and an HI leaving group. This was confirmed by IRC calculations and vibrational frequencies for the reaction coordinate were found to be $396i$, $319i$, and $151i\ cm^{-1}$, respectively, for TS1, TS2, and TS3. Examination of Fig. 8 reveals that as the number of H_2O molecules is increased, the degree of stabilization appears somewhat greater for the corresponding transition states and this leads to systematically lower barriers for reaction from the reactant complexes to the transition states: 13.6 kcal/mol from RC1 to TS1, 10.3 kcal/mol for RC2 to TS2, and 3.8 kcal/mol for RC3 to TS3. These results indicate that additional H_2O molecules substantially catalyze the CH_2I–I$+nH_2O\rightarrow CH_2I(OH)+HI+(n-1)H_2O$ ($n=1,2,3$) reaction. As the RCs proceed to the TSs, the I–I–C angle, I–I bond length, and C–O bond formation experience smaller changes as the number of H_2O molecules increases. For example, the I–I–C angle undergoes a change of 18° from RC1 to TS2, 13.6° from RC2 to TS2, and only 2.2° from RC3 to TS3. Similarly, the I–I bond length exhibits a change of 0.31 Å from RC1 to TS1, 0.23 Å from RC2 to TS2, and 0.146 Å from RC3 to TS3. The C–O bond formation is weaker (C–O bond lengths of 2.111 Å for TS1, 2.193 Å for TS2, and 2.386 Å for TS3. These changes in the I–I–C bond angle, I–I bond length, and C–O bond formation all suggest less energy is needed to go from the RCs to their TSs as more H_2O molecules are added. This is consistent with the

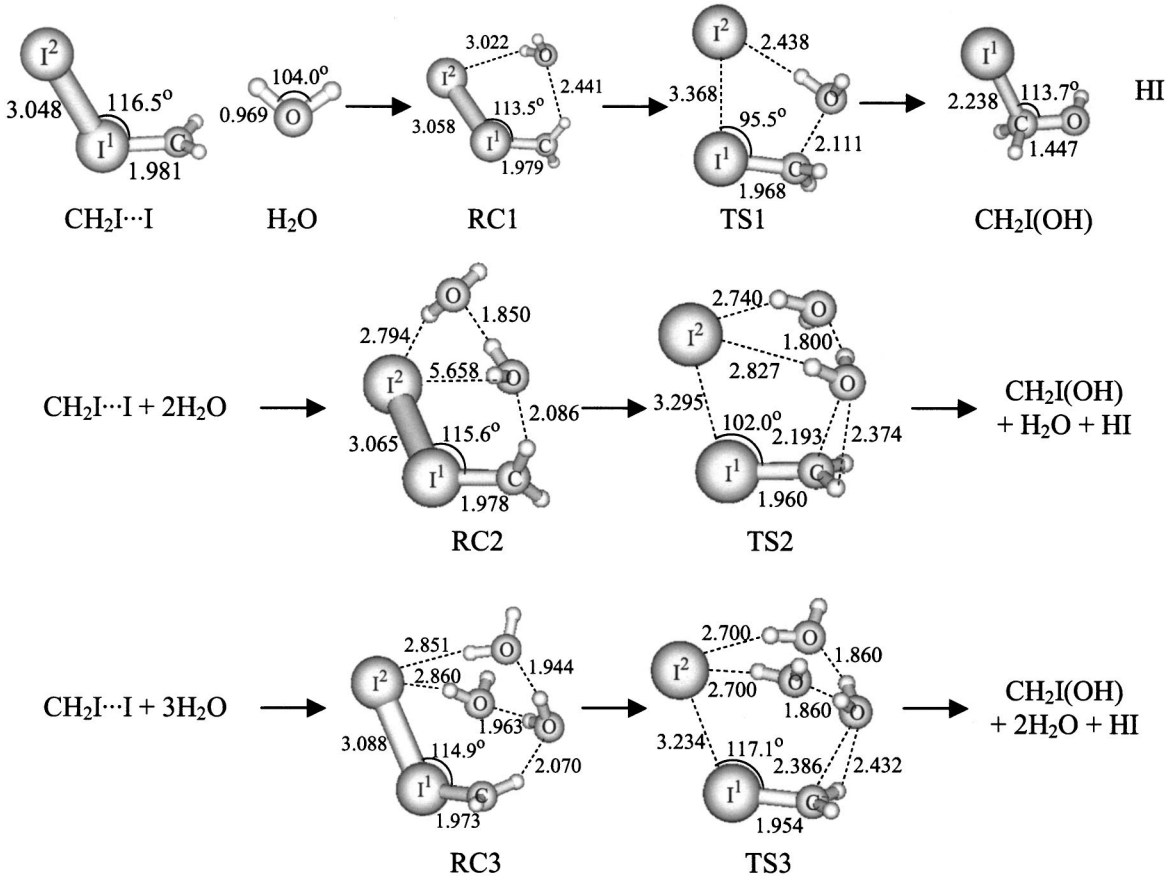

FIG. 6. Schematic diagrams are shown for the reactants, reactant complexes, transition states, product complexes, and products for the reactions of $CH_2I–I+nH_2O$ (where $n=1,2,3$). The optimized geometry for these species was obtained from MP2 calculations (using the 6-31G* basis set for all C, H, and O atoms and the 6-311G** basis set for iodide atoms). Selected bond length (in Å) and bond angle (in degrees) parameters are shown.

lower barriers to reaction observed (from 13.6 kcal/mol for RC1 to TS1 to only 3.8 kcal/mol from RC3 to TS3) as more H_2O molecules are involved in the reaction.

2. Reactions of $CH_2I(OH)+nH_2O$ (where $n=0,1,2,3,4$)

Inspection of Fig. 7 reveals that as the number of H_2O molecules increases in the reactant complexes, the O···H bond formed between a H_2O molecule and the H–O moiety of the $CH_2I(OH)$ molecule decreases from 1.807 Å for RC5 to 1.724 Å for RC6 to 1.647 Å for RC7 and then to 1.598 Å for RC8. This is accompanied by the bond of the H–O moiety of the $CH_2I(OH)$ molecule increase from 0.989 Å for RC5 to 1.001 Å for RC6 to 1.010 Å for RC7 and then to 1.020 Å for RC8. These results indicate that increasing the number of H_2O molecules systematically increases the strength of the hydrogen bonding to the H–O moiety of the $CH_2I(OH)$ molecule with water and weakens the strength of the H–O bond of the $CH_2I(OH)$ molecule. In the transition state structures, the C–I bond length decreases from 3.032 Å in TS4 to 2.634 Å in TS8 and the O–C–I angle increases from 103.7° in TS5 to 111.6° in TS8. The C–O bond length increases from 1.254 Å in TS5 to 1.282 Å in TS8. These changes in the TS structures can also be attributed to the solvation of the I atom with more hydrogen-bonding-like interactions while also interacting with the CH_2 group of the $CH_2I(OH)$ molecule via the O···H–C interaction.

The changes in structure in Fig. 7 occurring as the RCs proceed to the TSs indicate that the C–I bond becomes weaker, the O···H bond becomes partially formed in the O···H–O–C moiety of the $CH_2I(OH)$ molecule, and the I···H interactions generally become somewhat stronger, which is consistent with some H–I bond formation and with a HI-elimination reaction occurring to form an CH_2O product and an HI leaving group. This was confirmed by IRC calculations and vibrational frequencies for the reaction coordinate were found to be 551*i*, 501*i*, 570*i*, 407*i*, and 399*i* cm^{-1}, respectively, for TS4, TS5, TS6, TS7, and TS8. Examination of Fig. 8 shows the degree of stabilization appears greater for the corresponding transition states and this results in systematically lower barriers for reaction from the RCs to the TSs: 33.0 kcal/mol from RC4 to TS4, 14.0 kcal/mol from RC5 to TS5, 8.3 kcal/mol for RC6 to TS6, 4.0 kcal/mol for RC7 to TS7, and 3.4 kcal/mol for RC8 to TS8. This indicates that additional H_2O molecules substantially catalyze this reaction. As the RCs proceed to the TSs, the O–C–I angle, the C–O bond length, and the C–I bond length display smaller changes as the number of H_2O molecules increases. For example, the O–C–I angle undergoes a change of −9.5° from RC5 to TS5, −6.6° from RC6 to TS6, −3.8° from RC7 to TS7, and only 2° from RC8 to TS8. Similarly, the C–O bond length displays a change of −0.106 Å from RC5 to TS5, −0.103 Å from RC6 to TS6, −0.082 Å

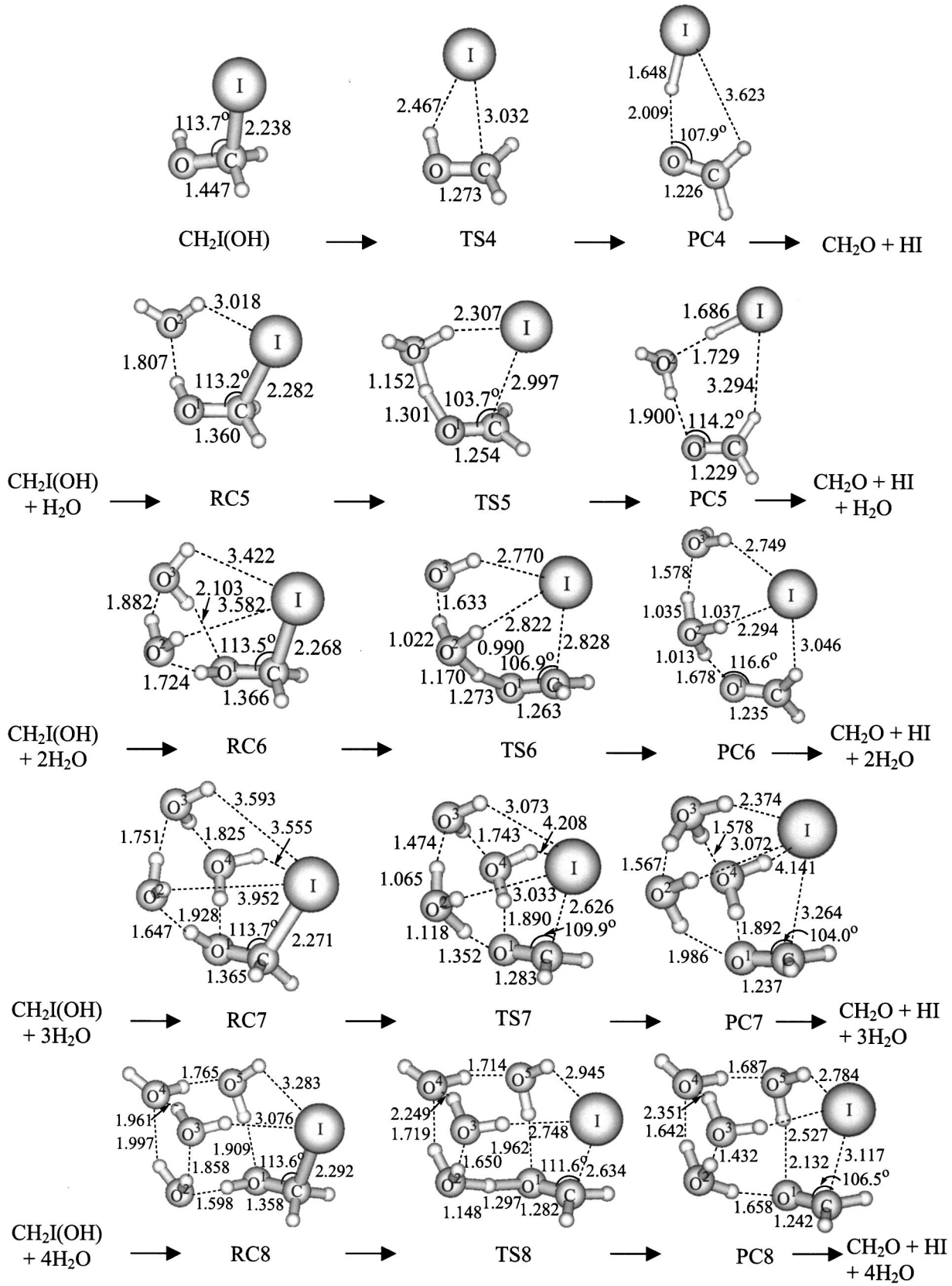

FIG. 7. Schematic diagrams are shown for the reactants, reactant complexes, transition states, product complexes, and products for the reactions of $CH_2I(OH) + nH_2O$ (where $n = 0,1,2,3,4$). The optimized geometry for these species was obtained from MP2 calculations (using the 6-31G* basis set for all C, H, and O atoms and the 6-311G** basis set for iodide atoms). Selected bond length (in Å) and bond angle (in degrees) parameters are shown.

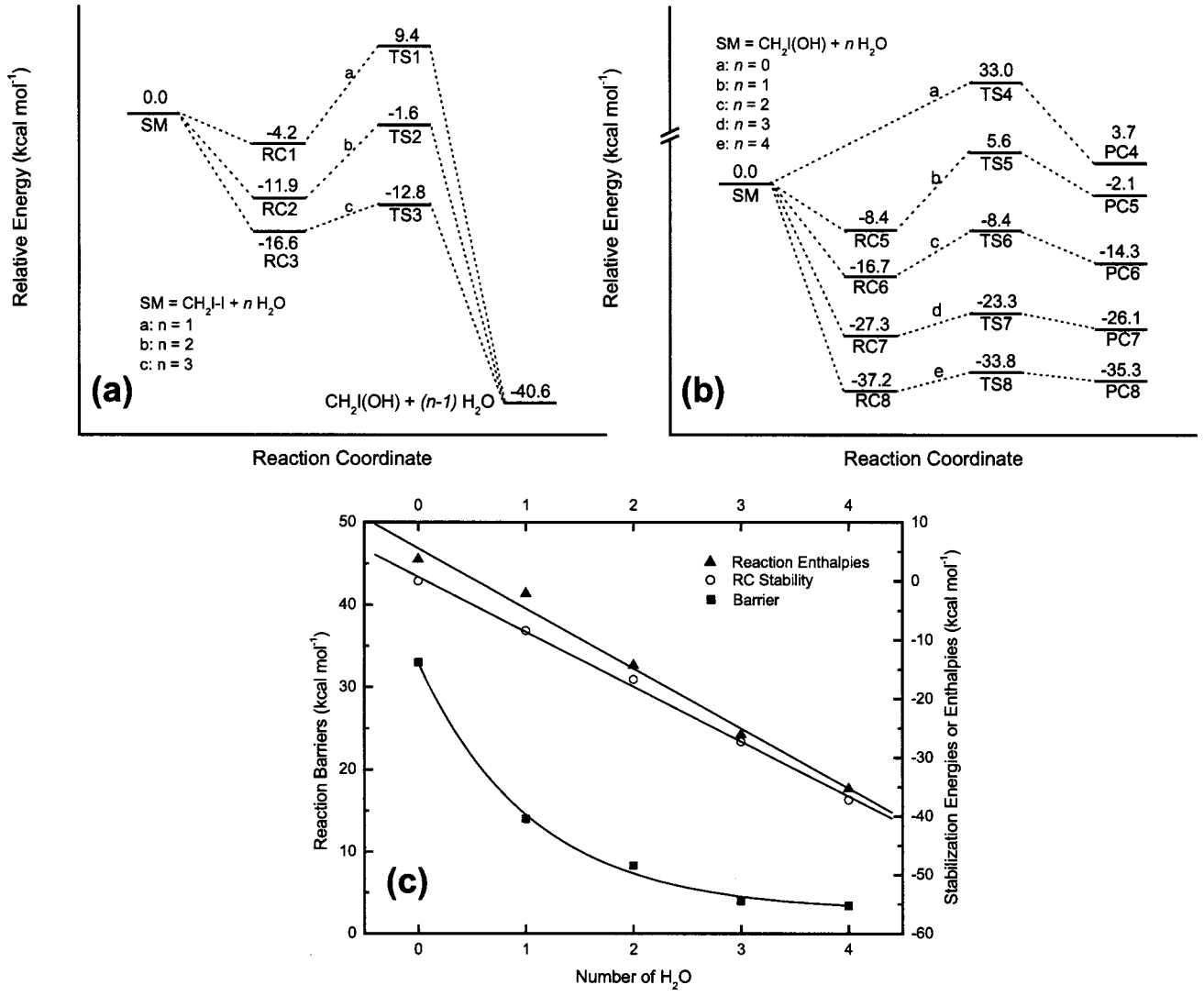

FIG. 8. (a) Schematic diagrams of the relative energy profiles (in kcal/mol) obtained from MP2 calculations (sing the 6-31G* basis set for all C, H, and O atoms and the 6-311G** basis set for iodide atoms) for the reactions of CH_2I–I+nH_2O (where $n=1,2,3$). (b) Schematic diagrams of the relative energy profiles (in kcal/mol) obtained from MP2 calculations (using the 6-31G* basis set for all C, H, and O atoms and the 6-311G** basis set for iodide atoms) for the reactions of $CH_2I(OH)+nH_2O$ (where $n=0,1,2,3,4$). (c) Plot of the stabilization energies (in kcal/mol) of both the reactant (open circles) and product (solid triangles) complexes and the barrier to reaction (solid squares) for the $CH_2I(OH)+nH_2O$ (where $n=1,2,3,4$) reactions as a function of the number of H_2O molecules. The lines give linear best fits to the stabilization energies of the reactant and product complexes and a best-fit exponential function to the barrier heights to the reactions as a function of the number of H_2O molecules.

from RC7 to TS7, and −0.076 Å from RC8 to TS8. The C–I bond show changes in the bond lengths of +0.715 Å from RC5 to TS5, +0.560 Å from RC6 to TS6, +0.355 Å from RC7 to TS7, and +0.342 Å from RC8 to TS8. These changes suggest less energy is needed to go from the RCs to their TSs as more H_2O molecules are added, consistent with the lower reaction barriers observed as more H_2O molecules are involved in the $CH_2I(OH)+nH_2O \rightarrow CH_2O+HI+nH_2O$ ($n=1,2,3,4$) reaction.

3. Water catalysis of the reactions of CH_2I–I+nH_2O (where $n=1,2,3$) and $CH_2I(OH)+nH_2O$ (where $n=0,1,2,3,4$) and solvation of the HI leaving group

It is interesting to compare our results to those previously found for neutral $I(H_2O)_n$ and $I^-(H_2O)_n$ complexes[123–125] as well as for the dissolution of strong acids (HX) by H_2O molecules.[126–131] For example, the stabilization energy of the I atom with H_2O is very weak and was computed[125] to be about 0.5 kcal/mol for I···HOH and 1.65 kcal/mol for I···OH_2 compared to the I^- anion with H_2O that was computed to be about −10.38 kcal/mol (Ref. 125) or −9.43 kcal/mol (Ref. 124). The stabilization energy of the $(CH_2I$–$I)H_2O$ and $[CH_2I(OH)]H_2O$ RCs were found to be 4.2 kcal/mol for RC1 and 8.4 kcal/mol for RC5, respectively. These values are between those found for the neutral $I(H_2O)_n$ and $I^-(H_2O)_n$ complexes[124,125] and suggest that solvation of the I^--like moiety occurs in the $(CH_2I$–$I)H_2O$ and $[CH_2I(OH)]H_2O$ RCs. Figure 8 shows a comparison of the stabilization energies of the RCs and the reaction enthalpies for the $CH_2I(OH)+nH_2O$ (where $n=0,1,2,3,4$) reactions plotted along with the relative energy for the barrier to reaction from the RCs to their respective TS as a function of H_2O molecules. The stabilization energies of the RCs and reaction enthalpies in Fig. 8 are fairly linear, while the bar-

rier to reaction exhibits an almost exponential decay due to greater stabilization of the TSs relative to the RCs as the H_2O molecules increase in number. The trends in the stabilization energies of the RCs for the $CH_2I–I+nH_2O$ (where $n=1,2,3$) and $CH_2I(OH)+nH_2O$ (where $n=1,2,3,4$) reactions are similar to previous results for solvation of an I^- anion by H_2O molecules[124,125] and consistent with solvation of an I^- like moiety in these reactions.

It is useful to compare our present results to those recently found for the dissociation of HI in H_2O complexes.[129] This study found that the stabilization energies of the $HI(H_2O)_n$ clusters varied from 4.02 kcal/mol for $n=1$ to 56.97 kcal/mol for $n=5$ similar to the trend found for the $I^-(H_2O)_n$ clusters[124,125] and our present results for the $(CH_2I–I)(H_2O)_n$ and $[CH_2I(OH)](H_2O)_n$ RCs and TSs in Figs. 7 and 8. The average H···I distances were found to be ~1.6 Å for $HI(H_2O)_n$ where $n=0,1,2$, ~2.1 Å for $HI(H_2O)_3$, and ~2.5 Å for $HI(H_2O)_n$ where $n=4,5$.[129] These results suggested that HI remains nondissociated with addition of one or two H_2O molecules, but becomes partially dissociated into a H_3O^+, I^- "ion-pair"-like species for the $HI(H_2O)_3$ complex and then is completely dissociated in the $HI(H_2O)_n$ where $n=4,5$ complexes.[129] The HI-elimination reactions of the $[CH_2I(OH)](H_2O)_n$ species are very similar to the dissociation of HI in the $HI(H_2O)_n$ species. Examination of the structures for the $(CH_2O)(HI)(H_2O)_n$ product complexes in Fig. 7 shows that PC4 with no H_2O molecule and PC5 with one H_2O molecule have H–I bond distances of 1.648 Å and 1.686 Å, respectively, which are close to the ~1.6 Å value for a nondissociated HI molecule. For the $(CH_2O)(HI)(H_2O)_n$ PCs with $n=2$ and 3, the H···I distances become intermediate in range with values of 2.294 Å for PC6 and 2.374 Å for PC7, consistent with partial dissociation into a H_3O^+, I^- "ion-pair"-like species similar to that found for the $HI(H_2O)_3$ complex.[129] For the $(CH_2O)\times(HI)(H_2O)_4$ product complex, the H···I distances become longer with values in the 2.5–2.7-Å range for PC8, consistent with complete dissociation into H_3O^+ and I^- species similar to that found for the $HI(H_2O)_n$ complexes where $n=4$ and 5.

An NBO analysis was done for the RCs, TSs, and PCs in Figs. 5–8. The terminal (or leaving) I atom has a NBO charge of −0.567 for RC1, −0.601 for RC2, and −0.655 for RC3 for the $CH_2I–I+nH_2O$ (where $n=1,2,3$) water-catalyzed O–H-insertion and HI-elimination reactions. The charges on the terminal I atom increases significantly as the RCs proceed to their respective TSs and have values of −0.829 for TS1, −0.844 for TS2, and −0.801 for TS3. The negative charges initially on the I atom of the $CH_2I(OH)$ molecule for the $CH_2I(OH)+nH_2O$ (where $n=0,1,2,3,4$) HI-elimination reactions are fairly small for their RCs with values of −0.045 for RC4, −0.145 for RC5, −0.124 for RC6, −0.130 for RC7, and −0.161 for RC8, but increase substantially in their respective TSs to −0.784 for TS4, −0.728 for TS5, −0.739 for TS6, −0.608 for TS7, and −0.600 for TS8. For both the $CH_2I–I+nH_2O$ (where $n=1,2,3$) and $CH_2I(OH)+nH_2O$ (where $n=0,1,2,3,4$) reactions the negative charge increases significantly from the RCs to their respective TSs with changes of charge of −0.262 from RC1 to TS1, −0.243 from RC2 to TS2, and −0.146 from RC3 to TS3 for the O–H-insertion/HI elimination reactions and −0.739 from RC4 to TS4, −0.583 from RC5 to TS5, −0.615 from RC6 to TS6, −0.478 from RC7 to TS7, and −0.439 from RC8 to TS8 for the HI-elimination reactions. As the number of H_2O molecules increases, there tends to be less change in the negative charge on the I atom as these reactions go from their RCs to their respective TS. This suggests that less energy is needed for redistribution of the charge to the I atom leaving group as the reaction goes from the RCs to their corresponding TSs. This behavior correlates with generally smaller structural changes and lower reaction barrier heights as the RCs go to their respective TSs as the number of H_2O molecules involved in these HI elimination reactions increases.

There are some interesting differences between the dissociation of HI in the $HI(H_2O)_n$ complexes and the water-catalyzed HI elimination reactions investigated here. For example, the proton is transferred from the HI molecule to the O atom of a water molecule in the dissociation of HI in the $HI(H_2O)_n$ complexes, while the proton is transferred from the OH group of the $CH_2I(OH)$ molecule in the $[CH_2I(OH)](H_2O)_n$ water-catalyzed HI-elimination reactions. This leads to the proton on the O–H group being shared with a H_2O molecule in the transition states (TS5–TS8) of the $[CH_2I(OH)](H_2O)_n$ water-catalyzed HI-elimination reactions. The HI-elimination and-dissociation processes in the $CH_2I–I(H_2O)_n$ reactions are coupled to the O–H insertion reaction with water and this results in the C–O bond formation of the H_2O molecule being coupled to a proton transfer to another H_2O molecule and the solvation of the terminal I atom (and cleavage of the I–I bond) of the $CH_2I–I$ species (see Fig. 6). This suggests that the water-catalyzed solvation and dissociation of a HI or similar leaving groups may be coupled to help drive other reactions for other potential synthetic applications. The ability of using water to catalyze other reactions by employing an appropriate leaving group(s) would probably be of general interest for synthetic chemists.

D. Proposed reaction mechanism for the $CH_2I_2+h\nu+n(H_2O)\rightarrow CH_2(OH)_2+2HI+(n-2)H_2O$ overall reaction

Based on our present experimental and theoretical results as well as other work already available in the literature, we propose the following reaction mechanism for the $CH_2I_2 + h\nu + n(H_2O) \rightarrow CH_2(OH)_2 + 2HI + (n-2)H_2O$ overall reaction that we observe for photolysis of low concentrations of CH_2I_2 in aqueous solutions:

Photolysis of CH_2I_2 *to form* CH_2I *and I fragments*:

Step 1 $CH_2I_2+h\nu\rightarrow CH_2I+I$.

Solvent-induced geminate recombination of the CH_2I *and I fragments to form the* $CH_2I–I$ *isomer*:

Step 2 $CH_2I+I\rightarrow CH_2I–I$.

Water-catalyzed O–H-*insertion and* HI-*elimination reaction of* $CH_2I–I$ *with* H_2O *solvent*:

Step 3 $CH_2I–I+n(H_2O)\rightarrow CH_2I(OH)+HI+(n-1)H_2O$.

Water-catalyzed HI-elimination reaction of $CH_2I(OH)$ *with* H_2O *solvent*:

Step 4 $CH_2I(OH)+n(H_2O)\rightarrow H_2CO+HI+n(H_2O)$.
Water (and/or acid) catalyzed addition of H_2O *to* H_2CO *in* H_2O *solvent*:
Step 5 $H_2CO+n(H_2O)\rightarrow CH_2(OH)_2+(n-1)H_2O$.
Add steps 1–5 to obtain this overall reaction:
$CH_2I_2+h\nu+n(H_2O)\rightarrow CH_2(OH)_2+2HI+(n-2)H_2O$.

It has been well established that ultraviolet excitation of CH_2I_2 in both gas and solution phases results in direct cleavage of the C–I bond to produce CH_2I radical and I atom fragments[42–58,77–79] and this indicates that step 1 in the above reaction mechanism is the primary photochemical start of the reaction. It has been clearly experimentally demonstrated that some of the initially produced CH_2I radical and I atom fragments can undergo solvent-induced geminate recombination to form a CH_2I–I isomer species within a few picoseconds[79,88] and this establishes that step 2 of the proposed reaction mechanism occurs to an appreciable extent in room-temperature solutions. Our ps-TR^3 experiments show that CH_2I–I is produced to an appreciable extent in largely aqueous solutions and has a substantially shorter lifetime with increasing water concentrations.[111] This suggests that CH_2I–I is reacting with H_2O molecules and is consistent with the proposed step 3 of the reaction mechanism. Previous experimental and theoretical studies[93–95] indicated the CH_2I–I species is an effective carbenoid species mostly responsible for the cyclopropanation of olefins when the ultraviolet photolysis of CH_2I_2 method is used. Other isopolyhalomethanes were also found to act as carbenoids with varying degrees of reactivity to olefins.[87,89,94,97] The chemical reactivity of CH_2I–I was found to be similar to that of singlet methylene towards C═C bonds in producing cyclopropanated products with high stereospecificity and little C–H-insertion products.[99,100] It is well known that carbenes and carbenoids such as singlet methylene[101–104,106–108] and dichlorocarbene ($:CCl_2$)[109,110] undergo O–H insertion reactions with water to produce CH_3OH and $CHCl_2OH$ products, respectively. Thus one may reasonably expect that the CH_2I–I carbenoid species probably can undergo similar reactions with H_2O. Our present *ab initio* study shows that this is indeed the case and CH_2I–I reacts with H_2O via a water-catalyzed O–H-insertion and HI-elimination reaction to produce $CH_2I(OH)$ and HI products and this is consistent with the proposed step 3 of the reaction mechanism. The $CH_2I(OH)$ and HI products do not absorb significantly at the 400-nm probe wavelength used in the ps-TR^3 experiments done in largely aqueous solutions[111] and thus would not likely be observed under these conditions, consistent with the ps-TR^3 results.[111] Recent ps-TR^3 experiments have demonstrated that the isobromoform (BrCHBr–Br) species reacts with water to directly produce the $CHBr_2(OH)$ product species.[122] This gives direct vibrational spectroscopic evidence that isopolyhalomethanes can undergo O–H-insertion reactions with H_2O molecules.[122] Insofar as the CH_2I–I species exhibits similar chemical reactivity, these experimental results for the isobromoform (BrCHBr–Br) species provide some experimental support for step 3 in our proposed reaction mechanism.

Our present *ab initio* study indicates that $CH_2I(OH)$ undergoes water-catalyzed HI elimination to produce H_2CO and HI products consistent with step 4 in our proposed reaction mechanism. Although not much is known about $CH_2I(OH)$, we note that the closely related chloromethanol [$CH_2Cl(OH)$] species has been observed in low-temperature matrix isolation experiments[132] and in gas-phase experiments[133,134] and in all cases was found to decompose in the dark to H_2CO and HCl products. The decomposition of chloromethanol [$CH_2Cl(OH)$] was accelerated by heterogenous processes in the gas-phase studies.[133,134] These experimental results are consistent with step 4 of our proposed reaction mechanism and our current *ab initio* results for the HI-elimination reaction of $CH_2I(OH)$ insofar as $CH_2I(OH)$ behaves like $CH_2Cl(OH)$.

It is well known experimentally that formaldehyde (H_2CO) in aqueous solution undergoes water addition to produce methanediol [$CH_2(OH)_2$].[116–118] This strongly supports step 5 in our proposed reaction mechanism in that any H_2CO produced in an aqueous environment will proceed to form methanediol [$CH_2(OH)_2$]. It is interesting to note that a theoretical investigation of this reaction indicates that this reaction may proceed mainly through a cooperative mechanism with three H_2O molecules hydrating the carbonyl group.[119] This cooperative mechanism is similar to the water-catalyzed CH_2I–I O–H-insertion and HI-elimination and $CH_2I(OH)$ HI-elimination reactions of steps 3 and 4 studied using MP2 *ab initio* methods in Sec. III C. The H_2CO product is produced with a nearby solvated HI leaving group in step 4 that could acid catalyze the water addition reaction of step 5. We expect that conversion of H_2CO to methanediol [$CH_2(OH)_2$] occurs very fast in aqueous solutions in the proposed reaction mechanism.

The proposed reaction mechanism here helps explain how photolysis of low concentrations of CH_2I_2 in aqueous solution leads to production of 2HI leaving groups and a $CH_2(OH)_2$ molecule as the main photolysis products observed by our ^{13}C-NMR, ^{1}H-NMR, IR, UV/VIS, and *p*H photochemistry results detailed in Sec. III A. Our present *ab initio* results indicate very low barriers to reaction for the water-catalyzed CH_2I–I O–H-insertion and HI-elimination (predicted barrier of only 3.8 kcal/mol from RC3 to TS3 for the reaction with three water molecules involved) and $CH_2I(OH)$ HI-elimination (predicted barrier of only 3.4 kcal/mol from RC8 to TS8 for the reaction with four water molecules involved) reactions of steps 3 and 4. This and the known chemistry of H_2CO in aqueous solutions for step 5 indicate that the very reactive CH_2I–I species would likely be efficiently converted into the 2HI and $CH_2(OH)_2$ final products. This is consistent with the efficient photoconversion of the CH_2I_2 molecule into the 2HI and $CH_2(OH)_2$ final products and a fairly high photochemical quantum yield for this overall dehalogenation reaction (estimated to be about 0.35).

E. Discussion of the water-catalyzed O–H-insertion and HI-elimination reactions and likely implications for decomposition of polyhalomethanes and halomethanols in aqueous environments

The ultraviolet photolysis of CH_2I_2 in the gas phase leads predominantly to a direct C–I bond cleavage and for-

mation of CH_2I radical and I fragments with a near-unity photon quantum yield.[42–44] However, we found that ultraviolet photolysis of CH_2I_2 at low concentrations in aqueous solution leads to conversion of the parent molecule into 2HI and $CH_2(OH)_2$ stable products with about a 0.35 photon quantum yield. These results indicate that the photochemistry of CH_2I_2 exhibits significant phase dependence with very different reactions taking place in aqueous solution compared to the gas phase. The reaction mechanism proposed in Sec. III C that involves the O–H-insertion and HI-elimination reactions of CH_2I–I with water and the HI-elimination reaction of $CH_2I(OH)$ with water combined with the known chemistry of formaldehyde in water can account for how ultraviolet photolysis of CH_2I_2 in aqueous solution can undergo dehalogenation to make 2HI and $CH_2(OH)_2$ products. These water-catalyzed reactions of CH_2I–I with water and the subsequent HI-elimination reaction of $CH_2I(OH)$ with water may be noticeable sources of halogens and/or acid formation in the atmosphere. The water-catalyzed reactions of isopolyhalomethanes like CH_2I–I have not been considered to our knowledge for the water solvated photochemistry of polyhalomethanes that have been observed in the natural environment from natural and/or man-made sources.[1–8]

We have recently used ps-TR^3 experiments to observe appreciable formation of isopolyhalomethanes (like CH_2I–I and BrCHBr–Br) in mixed aqueous solutions. In the case of isobromoform (BrCHBr–Br), we were able to directly observe its O–H-insertion reaction with water to form a $CHBr_2(OH)$ product.[122] We note that photolysis of a number of polyhalomethanes in condensed-phase media has been found to produce noticeable amounts of isopolyhalomethanes[73,74,77–92] and it is likely that a range of isopolyhalomethanes can be formed in noticeable quantities in aqueous solvents as observed for other solvent systems. Insofar as other isopolyhalomethanes exhibit similar chemical reactivity with water as the CH_2I–I species, we expect that photolysis of polyhalomethanes in solvated water environments would release significant amounts of HX strong acid leaving groups. This suggests that the pH in the solvated aqueous environment around the parent polyhalomethane becomes more acidic and may significantly influence reactions associated with the activation of halogens in aqueous sea-salt particles since many reaction schemes presented depend on pH.[10–21] For halogen activation on aqueous sea-salt particles, key reactions have been proposed where H^+ and X^- help activate the halogen atom (these studies typically focused on release of bromine and/or chlorine).[10–21] Reaction schemes have proposed $HOX + H^+ + X^- \rightarrow X_2 + H_2O$ (where X=Cl and/or Br) and/or $HOX^- + H^+ \rightarrow X + H_2O$ as a key step(s) in the halogen activation process.[10–20]

Our present work indicates that photolysis of CH_2I_2 in aqueous solution releases two HI groups. We speculate that if this happens in aqueous sea-salt particles, the HI released may cause analogous reactions to activate halogens such as by the $HOX + H^+ + I^- \rightarrow XI + H_2O$ reaction. If X is Cl or Br, then the activation of I would be accompanied by Cl or Br and likely cause additional ozone destruction via their known synergistic pathways. Photolysis of CH_2BrI in aqueous solution produces both HBr and HI similar to producing 2HI groups from ultraviolet photolysis of CH_2I_2 studied here.[135] We also found that ultraviolet photolysis of CH_3I in aqueous solution does not release noticeable acid groups[135] and this is probably due to its inability to make an isopolyhalomethane from its two initially produced photofragments in the condensed phase. We note that the photochemistry of CH_2I_2 and CH_2BrI was found to be responsible for most of the IO observed in the marine boundary layer of the troposphere.[7,8] However, CH_3I made very little contribution even though it is present in greater amounts (mean concentration of 0.43 pptv compared to 0.08 and 0.05 pptv for CH_2I_2 and CH_2BrI, respectively).[7,8] We speculate that the aqueous-phase photochemistry of CH_2I_2 and CH_2BrI that releases strong acids with the potential for halogen activation in sea-salt particles may possibly account for why the photochemistry of CH_2I_2 and CH_2BrI are mainly responsible for the formation of IO in the marine boundary layer, while the CH_3I molecule (which does not have the isopolyhalomethane chemistry and its strong acid release) does not have much of a contribution to IO production. We have observed that ultraviolet photolysis of several polyhalomethanes in aqueous solutions releases strong acids with reasonable quantum yields[133] via their isopolyhalomethane chemistry. Thus we feel it would be worthwhile to pursue additional studies to better understand how this water-solvated chemistry may actually influence or affect the chemistry of the atmosphere, particularly for reactions that are acid catalyzed or affected by pH such as halogen activation in heterogeneous environments.

Halomethanols like bromomethanol and chloromethanol can be formed in the atmosphere by reaction of hydroxymethyl radicals (CH_2OH) with atomic or molecular halogens in the gas phase and may possibly act as a halogen reservoir in the atmosphere.[9,130,136,137] Chloromethanol was found to decompose into HCl and H_2CO products and have a lifetime of at least a 100 s (and probably much longer) due to homogeneous decomposition in the gas phase.[133,134] Chloromethanol was also found to decay much faster on surfaces.[133,134] Our present *ab initio* results for the reaction of iodomethanol [$CH_2I(OH)$] indicate that the decomposition of halomethanols can be greatly accelerated by even a reaction with one water molecule and further accelerated by additional H_2O molecules. This suggests that decomposition of halomethanols will be very sensitive to the humidity of the atmosphere and rapidly decomposes in solvated water environments (such as the interfacial and/or bulk regions of water and ice particles). It would appear to be prudent to investigate the reaction rates for halomethanols with H_2O in the gas phase, on surfaces, and in bulk aqueous solutions to better understand their decomposition in the atmosphere. Our present *ab initio* work for the CH_2I–I reactions with water and our recent direct observation of the O–H insertion reaction of isobromoform to produce the $CHBr_2OH$ molecule indicate that halomethanols can be produced in appreciable amounts due to the photochemistry of polyhalomethanes in solvated aqueous environments. This new photochemical route to produce halomethanols could be exploited to explore the relatively unknown chemistry of halomethanols in condensed-phase environments.

IV. CONCLUSION

Photochemistry experiments were shown that observe ultraviolet photolysis of low concentrations of CH_2I_2 in water leads to almost complete conversion into $CH_2(OH)_2$ and 2HI products. *Ab initio* calculations showed the CH_2I–I species can react readily with water via a water-catalyzed O–H-insertion and HI-elimination reaction to produce $CH_2I(OH)$ + HI. This $CH_2I(OH)$ product then undergoes a further water-catalyzed HI elimination reaction to form $H_2O{=}O$ + HI. These HI-elimination reactions make the two HI leaving groups seen in the photochemistry experiments. The $H_2C{=}O$ product further reacts with water to form the other final $CH_2(OH)_2$ product seen in the photochemistry experiments. These results combined with the experimental observation of CH_2I–I in largely aqueous solutions indicate CH_2I–I reacts with water to produce the $CH_2(OH)_2$ and 2HI products observed in the low-concentration-CH_2I_2 photochemistry experiments. A reaction mechanism was proposed that is consistent with our present experimental and theoretical results as well as with other experimental results.

Our *ab initio* calculations showed systematic changes in the structures and relative energies of the RCs, TSs, and PCs for the CH_2I–I+$n$$H_2O$ (where $n=1,2,3$) and $CH_2I(OH)$ + $n$$H_2O$ (where $n=0,1,2,3,4$) reactions consistent with increasing solvation of the H*X* leaving group as the number of H_2O molecules increase. Both reactions exhibited a significant increase in charge as one goes from their RCs to their respective TSs. This occurred with less change in the negative charge of the I atom as these reactions go from their RCs to their respective TS as the number of H_2O molecules increases. This suggests that less energy is needed for a redistribution of the charge to the I atom leaving group as the reaction goes from their RCs to their corresponding TSs. This correlates with smaller structural changes and lower reaction barrier heights as the RCs go to their respective TSs as the number of H_2O molecules involved in the reaction increases for the CH_2I–I+$n$$H_2O$ and $CH_2I(OH)$+$n$$H_2O$ reactions and indicates that these reactions are water-catalyzed reactions driven by solvation of the HI leaving group.

Our present study demonstrates that ultraviolet photolysis of CH_2I_2 at low concentration leads to efficient dehalogenation and release of multiple strong acid (HI) leaving groups. At present, it is not known how this water-solvated chemistry may actually influence or affect the chemistry of the natural environment. This is particularly true for reactions that are acid catalyzed or affected by *p*H such as halogen activation in heterogeneous environments and much further research is needed to assess the potential impact of the water-catalyzed isopolyhalomethane reactions in the natural environment. This may prove to be an active and interesting area of research.

ACKNOWLEDGMENTS

This research has been supported by grants from the Research Grants Council of Hong Kong (Nos. HKU/7087/01P and HKU 1/01C) to D.L.P. W.M.K. would like to thank the University of Hong Kong for the award of a Postdoctoral Fellowship.

[1] Th. Class and K. Ballschmiter, J. Atmos. Chem. **6**, 35 (1988).
[2] S. Klick and K. Abrahamsson, J. Geophys. Res. **97**, 12683 (1992).
[3] K. G. Heumann, Anal. Chim. Acta **283**, 230 (1993).
[4] R. M. Moore, M. Webb, R. Tokarczyk, and R. Wever, J. Geophys. Res., [Oceans] **101**, 20899 (1996).
[5] C. T. McElroy, C. A. McLinden, and J. C. McConnell, Nature (London) **397**, 338 (1997).
[6] J. C. Mössigner, D. E. Shallcross, and R. A. Cox, J. Chem. Soc., Faraday Trans. **94**, 1391 (1998).
[7] L. J. Carpenter, W. T. Sturges, S. A. Penkett, and P. S. Liss, J. Geophys. Res., [Atmos.] **104**, 1679 (1999).
[8] B. Alicke, K. Hebstreit, J. Stutz, and U. Platt, Nature (London) **397**, 572 (1999).
[9] R. P. Wayne, *Chemistry of Atmospheres*, 3rd ed. (Oxford University Press, Oxford, 2000).
[10] S.-F. Fan and D. J. Jacob, Nature (London) **359**, 522 (1992).
[11] M. Mozurkewich, J. Geophys. Res. **100**, 14199 (1995).
[12] R. Vogt, P. J. Crutzen, and S. Sander, Nature (London) **383**, 327 (1996).
[13] R. Sander and P. J. Crutzen, J. Geophys. Res. **101**, 9121 (1996).
[14] K. W. Oum, M. J. Lakin, D. O. DeHaan, T. Brauers, and B. J. Finalyson-Pitts, Science **279**, 74 (1998).
[15] C. T. McElroy, C. A. McLinden, and J. C. McConnell, Nature (London) **397**, 338 (1999).
[16] R. Vogt, R. Sander, R. V. Glasow, and P. J. Crutzen, J. Atmos. Chem. **32**, 375 (1999).
[17] W. Behnke, M. Elend, U. Krüger, and C. Zetzsch, J. Atmos. Chem. **34**, 87 (1999).
[18] E. M. Knipping, M. J. Lakin, K. L. Foster, P. Jungwirth, D. J. Tobias, R. B. Gerber, D. Dabdub, and B. J. Finalyson-Pitts, Science **288**, 301 (2000).
[19] B. J. Finalyson-Pitts, and J. C. Hemminger, J. Phys. Chem. A **104**, 11463 (2000).
[20] K. L. Foster, R. A. Plastridge, J. W. Bottenheim, P. B. Shepson, B. J. Finalyson-Pitts, and C. W. Spicer, Science **291**, 471 (2001).
[21] X.-Y. Yu and J. R. Barker, J. Phys. Chem. A **107,** 1313 (2003).
[22] H. E. Simmons and R. D. Smith, J. Am. Chem. Soc. **81**, 4256 (1959).
[23] D. C. Blomstrom, K. Herbig, and H. E. Simmons, J. Org. Chem. **30**, 959 (1965).
[24] R. C. Neunman, Jr. and R. G. Wolcott, Tetrahedron Lett. **7**, 6267 (1966).
[25] T. Marolewski and N. C. Yang, J. Chem. Soc., Chem. Commun. **23**, 1225 (1967).
[26] N. C. Yang and T. A. Marolewski, J. Am. Chem. Soc. **90**, 5644 (1968).
[27] S. Sawada, J. Oda, and Y. Iouye, J. Org. Chem. **33**, 2141 (1968).
[28] J. Furukawa, N. Kawabata, and J. Nishimura, Tetrahedron **24**, 53 (1968).
[29] C. D. Poulter, E. C. Friedrich, and S. Winstein, J. Am. Chem. Soc. **91**, 6892 (1969).
[30] H. E. Simmons, T. L. Cairns, S. A. Vladuchick, and C. M. Hoiness, Org. React. (N.Y.) **20**, 1 (1973).
[31] N. Kawabata, T. Nakagawa, T. Nakao, and S. Yamashita, J. Org. Chem. **42**, 3031 (1977).
[32] N. J. Pienta and P. J. Kropp, J. Am. Chem. Soc. **100**, 655 (1978).
[33] P. J. Kropp, N. J. Pienta, J. A. Sawyer, and R. P. Polniaszek, Tetrahedron **37**, 3229 (1981).
[34] R. D. Rieke, T.-J. Li, T. P. Burns, and S. T. Uhm, J. Org. Chem. **46**, 4323 (1981).
[35] P. J. Kropp, Acc. Chem. Res. **17**, 131 (1984).
[36] K. Maruoka, Y. Fukutani, and H. Yamamoto, J. Org. Chem. **50**, 4412 (1985).
[37] E. C. Friedrich, J. M. Domek, and R. Y. Pong, J. Org. Chem. **50**, 4640 (1985).
[38] E. C. Friedrich, S. E. Lunetta, and E. J. Lewis, J. Org. Chem. **54**, 2388 (1989).
[39] G. A. Molander and L. S. Harring, J. Org. Chem. **54**, 3525 (1989).
[40] S. Durandetti, S. Sibille, and J. Périchon, J. Org. Chem. **56**, 3255 (1991).
[41] A. B. Charette and A. Beauchemin, Org. React. (N.Y.) **58**, 1 (2001).
[42] M. Kawasaki, S. J. Lee, and R. Bersohn, J. Chem. Phys. **63**, 809 (1975).
[43] G. Schmitt and F. J. Comes, J. Photochem. **14**, 107 (1980).
[44] P. M. Kroger, P. C. Demou, and S. J. Riley, J. Chem. Phys. **65**, 1823 (1976).
[45] J. B. Koffend and S. R. Leone, Chem. Phys. Lett. **81**, 136 (1981).
[46] S. R. Cain, R. Hoffman, and R. Grant, J. Phys. Chem. **85**, 4046 (1981).
[47] S. J. Lee and R. Bersohn, J. Phys. Chem. **86**, 728 (1982).
[48] L. J. Butler, E. J. Hintsa, and Y. T. Lee, J. Chem. Phys. **84**, 4104 (1986).
[49] L. J. Butler, E. J. Hintsa, and Y. T. Lee, J. Chem. Phys. **86**, 2051 (1987).

[50] E. A. J. Wannenmacher, P. Felder, and J. R. Huber, J. Chem. Phys. **95**, 986 (1991).
[51] G. Baum, P. Felder, and J. R. Huber, J. Chem. Phys. **98**, 1999 (1993).
[52] U. Marvet and M. Dantus, Chem. Phys. Lett. **256**, 57 (1996).
[53] Q. Zhang, U. Marvet, and M. Dantus, J. Chem. Phys. **109**, 4428 (1998).
[54] K.-W. Jung, T. S. Ahmadi, and M. A. El-Sayed, Bull. Korean Chem. Soc. **18**, 1274 (1997).
[55] W. Radloff, P. Farmanara, V. Stert, E. Schreiber, and J. R. Huber, Chem. Phys. Lett. **291**, 173 (1998).
[56] K. Kavita and P. K. Das, J. Chem. Phys. **112**, 8426 (2000).
[57] S. L. Baughcum, H. Hafmann, S. R. Leone, and D. Nesbitt, Faraday Discuss. Chem. Soc. **67**, 306 (1979).
[58] S. L. Baughcum and S. R. Leone, J. Chem. Phys. **72**, 6531 (1980).
[59] J. Zhang and D. G. Imre, J. Chem. Phys. **89**, 309 (1988).
[60] W. M. Kwok and D. L. Phillips, Chem. Phys. Lett. **235**, 260 (1995).
[61] W. M. Kwok and D. L. Phillips, Chem. Phys. Lett. **241**, 267 (1995).
[62] S. Q. Man, W. M. Kwok, and D. L. Phillips, J. Phys. Chem. **99**, 15705 (1995).
[63] W. M. Kwok and D. L. Phillips, J. Chem. Phys. **104**, 2529 (1996).
[64] W. M. Kwok and D. L. Phillips, J. Chem. Phys. **104**, 9816 (1996).
[65] S. Q. Man, W. M. Kwok, A. E. Johnson, and D. L. Phillips, J. Chem. Phys. **105**, 5842 (1996).
[66] F. Duschek, M. Schmitt, P. Vogt, A. Materny, and W. Kiefer, J. Raman Spectrosc. **28**, 445 (1997).
[67] M. Braun, A. Materny, M. Schmitt, W. Kiefer, and V. Engel, Chem. Phys. Lett. **284**, 39 (1998).
[68] X. Zheng and D. L. Phillips, Chem. Phys. Lett. **313**, 467 (1999).
[69] D. L. Phillips, Prog. React. Kinet. Mech. **24**, 223 (1999).
[70] J. P. Simons and P. E. R. Tatham, J. Chem. Soc. A. **1966**, 854.
[71] L. Andrews, F. T. Prochaska, and B. S. Ault, J. Am. Chem. Soc. **101**, 9 (1979).
[72] H. Mohan, K. N. Rao, and R. M. Iyer, Radiat. Phys. Chem. **23**, 505 (1984).
[73] G. Maier and H. P. Reisenauer, Angew. Chem., Int. Ed. Engl. **25**, 819 (1986).
[74] G. Maier, H. P. Reisenauer, J. Lu, L. J. Scaad, and B. A. Hess, Jr., J. Am. Chem. Soc. **112**, 5117 (1990).
[75] H. Mohan and R. M. Iyer, Radiat. Eff. **39**, 97 (1978).
[76] H. Mohan and P. N. Moorthy, J. Chem. Soc., Perkin Trans. 2 **2**, 277 (1990).
[77] B. J. Schwartz, J. C. King, J. Z. Zhang, and C. B. Harris, Chem. Phys. Lett. **203**, 503 (1993).
[78] K. Saitow, Y. Naitoh, K. Tominaga, and Y. Yoshihara, Chem. Phys. Lett. **262**, 621 (1996).
[79] A. N. Tarnovsky, J.-L. Alvarez, A. P. Yartsev, V. Sündstrom, and E. Åkesson, Chem. Phys. Lett. **312**, 121 (1999).
[80] A. N. Tarnovsky, M. Wall, M. Rasmusson, T. Pascher, and E. Åkesson, J. Chin. Chem. Soc. (Taipei) **47**, 769 (2000).
[81] A. N. Tarnovsky, M. Wall, M. Gustafsson, N. Lascoux, V. Sundström, and E. Åkesson, J. Phys. Chem. A **106**, 5999 (2002).
[82] M. Wall, A. N. Tarnovsky, T. Pascher, V. Sundström, and E. Åkesson, J. Phys. Chem. A **107**, 211 (2003).
[83] X. Zheng and D. L. Phillips, Chem. Phys. Lett. **324**, 175 (2000).
[84] X. Zheng and D. L. Phillips, J. Chem. Phys. **113**, 3194 (2000).
[85] X. Zheng and D. L. Phillips, J. Phys. Chem. A **104**, 6880 (2000).
[86] X. Zheng, W. M. Kwok, and D. L. Phillips, J. Phys. Chem. A **104**, 10464 (2000).
[87] X. Zheng, W.-H. Fang, and D. L. Phillips, J. Chem. Phys. **113**, 10934 (2000).
[88] W. M. Kwok, C. Ma, A. W. Parker, D. Phillips, M. Towrie, P. Matousek, and D. L. Phillips, J. Chem. Phys. **113**, 7471 (2000).
[89] X. Zheng, C. W. Lee, Y.-L. Li, W.-H. Fang, and D. L. Phillips, J. Chem. Phys. **114**, 8347 (2001).
[90] W. M. Kwok, C. Ma, A. W. Parker, D. Phillips, M. Towrie, P. Matousek, X. Zheng, and D. L. Phillips, J. Chem. Phys. **114**, 7536 (2001).
[91] W. M. Kwok, C. Ma, A. W. Parker, D. Phillips, M. Towrie, P. Matousek, and D. L. Phillips, Chem. Phys. Lett. **341**, 292 (2001).
[92] Y.-L. Li, D. Wang, and D. L. Phillips, Bull. Chem. Soc. Jpn. **75**, 943 (2002).
[93] D. L. Phillips, W.-H. Fang, and X. Zheng, J. Am. Chem. Soc. **123**, 4197 (2001).
[94] D. L. Phillips, and W.-H. Fang, J. Org. Chem. **66**, 5890 (2001).
[95] Y.-L. Li, K. H. Leung, and D. L. Phillips, J. Phys. Chem. A **105**, 10621 (2001).
[96] W.-H. Fang, D. L. Phillips, D. Wang, and Y.-L. Li, J. Org. Chem. **67**, 154 (2002).
[97] Y.-L. Li, D. M. Chen, D. Wang, and D. L. Phillips, J. Org. Chem. **67**, 4228 (2002).
[98] Y.-L. Li, D. Wang, and D. L. Phillips, J. Chem. Phys. **117**, 7931 (2002).
[99] B. Zurawski and W. Kutzelnigg, J. Phys. Chem. A **100**, 2654 (1978).
[100] S. Sakai, Int. J. Quantum Chem. **70**, 291 (1998).
[101] L. B. Harding, H. B. Schlegel, R. Krishnan, and J. A. Pople, J. Phys. Chem. **84**, 3394 (1980).
[102] J. A. Pople, K. Raghavachari, M. J. Frisch, J. B. Blinkley, and P. V. R. Schleyer, J. Am. Chem. Soc. **105**, 6389 (1983).
[103] C. Wesdemiotis, R. Feng, P. O. Danis, E. R. Williams, and F. W. Lafferty, J. Am. Chem. Soc. **108**, 5847 (1986).
[104] B. F. Yates, W. J. Bouma, and L. Radom, J. Am. Chem. Soc. **109**, 2250 (1987).
[105] W. Kirmse, T. Meinert, D. A. Moderelli, and M. S. Platz, J. Am. Chem. Soc. **115**, 8918 (1993).
[106] S. P. Walch, J. Chem. Phys. **98**, 3163 (1993).
[107] C. Gonzalez, A. Restrepo-Cossio, M. Márquez, and K. B. Wiberg, J. Am. Chem. Soc. **118**, 5408 (1996).
[108] C. J. Moody and G. H. Whitman, in *Reactive Intermediates*, edited by S. G. Davies (Oxford University Press, New York, 1992).
[109] J. R. Pliego, Jr. and W. B. De Almeida, J. Phys. Chem. **100**, 12410 (1996).
[110] J. R. Pliego, Jr. and W. B. De Almeida, J. Phys. Chem. A **103**, 3904 (1999).
[111] W. M. Kwok, C. Ma, A. W. Parker, D. Phillips, M. Towrie, P. Matousek, and D. L. Phillips, J. Phys. Chem. A **107**, 2624 (2003).
[112] Y.-L. Li, C. Y. Zhao, W. M. Kwok, X. G. Guan, P. Zuo, and D. L. Phillips, J. Chem. Phys. **119**, 4671 (2003).
[113] M. J. Frisch, G. W. Trucks, H. B. Schlegel, GAUSSIAN 98, Revision A.7, Gaussian, Inc., Pittsburgh, PA, 1998.
[114] C. Gonzalez and H. B. Schlegel, J. Chem. Phys. **90**, 2154 (1989); J. Phys. Chem. **94**, 5523 (1990).
[115] See EPAPS document no. E-JCPSA6-120-015418 for supporting information on the Cartesian coordinates, total energies and vibrational zero-point energies for selected stationary structures shown in Figs. 5 and 6. A direct link to this document may be found in the online article's HTML reference section. The document may also be reached via the EPAPS homepage (http://www.aip.org/pubservs/epaps.html) or from ftp.aip.org in the directory /epaps/. See the EPAPS homepage for more information.
[116] D. J. Le Botlan, B. J. Mechin, and G. J. Martin, Anal. Chem. **55**, 587 (1983).
[117] R. P. Bell, Adv. Phys. Org. Chem. **4**, 1 (1966).
[118] A. A. Zavitsas, M. Coffiner, T. Wiseman, and L. R. Zavitsas, J. Phys. Chem. **74**, 2746 (1970).
[119] S. Wolfe, C.-K. Kim, K. Yang, N. Weinberg, and Z. Shi, J. Am. Chem. Soc. **117**, 4240 (1995).
[120] I. Nicole, J. De Laat, M. Dore, J. P. Duguet, and H. Et Suty, Environ. Sci. Technol. **12**, 21 (1991).
[121] A. N. Tarnovsky, V. Sundstrom, E. Akesson, and T. Pascher, J. Phys. Chem. A **108**, 237 (2004).
[122] W. M. Kwok, C. Y. Zhao, Y.-L. Li, X. G. Guan, and D. L. Phillips, J. Phys. Chem. **120**, 3323 (2004).
[123] U. Achatz, B. S. Fox, M. K. Beyer, and V. E. Bondybey, J. Am. Chem. Soc. **123**, 6151 (2001).
[124] H. M. Lee and K. S. Kim, J. Chem. Phys. **114**, 4461 (2001).
[125] M. Kowal, R. W. Gora, S. Roszak, and J. Lexzczynski, J. Chem. Phys. **115**, 9260 (2001).
[126] C. Conley and F.-M. Tao, Chem. Phys. Lett. **301**, 29 (1999).
[127] B. J. Gertner, G. H. Peslherbe, and J. T. Hynes, Isr. J. Chem. **39**, 273 (1999).
[128] A. Milet, C. Struniewicz, R. Moszynski, and P. E. S. Wormer, J. Chem. Phys. **115**, 349 (2001).
[129] E. M. Cabaleiro-Lago, J. M. Hermida-Ramón, and J. Rodríguez-Otero, J. Chem. Phys. **117**, 3160 (2002).
[130] S. M. Hurley, T. E. Dermota, D. P. Hydutsky, and A. W. Castleman, Jr., Science **298**, 202 (2002).

[131] A. F. Voegele and K. R. Liedl, Angew. Chem., Int. Ed. Engl. **42**, 2114 (2003).
[132] H. Knuttu, M. Dahlqvist, J. Murto, and M. Räsänen, J. Phys. Chem. **92**, 1495 (1988).
[133] G. S. Tyndall, T. J. Wallington, M. D. Hurley, and W. F. Schneider, J.Phys. Chem. **97**, 1576 (1993).
[134] T. J. Wallington, W. F. Schneider, I. Barnes, K. H. Becker, J. Sehested, and O. J. Nielsen, Chem. Phys. Lett. **322**, 97 (2000).
[135] W. M. Kwok, C. Zhao, Y.-L. Li, X. Guan, and D. L. Phillips (unpublished).
[136] H. H. Grotheer, G. Riekert, U. Meier, and Th. Just, in Proceedings of the International Symposium on Gas Kinetics, Bordeaux, France, 1986 (unpublished).
[137] M. E. Jenkin, R. A. Cox, G. D. Hayman, and L. J. Whyte, J. Chem. Soc., Perkin Trans. 2 **84**, 913 (1988).